DOCTORAL DISSERTATION SERIES

TITLE THE EFFECT OF PRESSURE ON THE DEHYDRATION OF BUTANOL-1 OVER AN ALUMINA-SILICA CATALYST

AUTHOR JOHN FREDERICK MAURER

UNIVERSITY OF MICH.

DATE 1950

DEGREE Ph. D. PUBLICATION NO. 3532

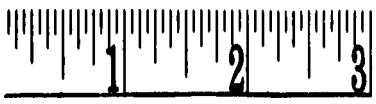

UNIVERSITY MICROFILMS
ANN ARBOR · MICHIGAN

THE EFFECT OF PRESSURE ON THE DEHYDRATION OF BUTANOL-1 OVER AN ALUMINA-SILICA CATALYST

by

John Frederick Maurer

A dissertation submitted in partial fulfillment
of the requirements for the degree of
Doctor of Philosphy in the
University of Michigan
1950

Committee in charge:

Assistant Professor C. M. Sliepcevich, Chairman
Professor George Granger Brown
Associate Professor J. W. Freeman
Assistant Professor P. A. S. Smith
Professor R. R. White

To My Parents

STATEMENT OF THE PROBLEM

The purpose of this investigation was to study the effect of pressure on the initial rate of dehydration of butanol-1 over an alumina-silica catalyst at 750° Fahrenheit.

ACKNOWLEDGMENT

The author expresses his appreciation to all those who have directly or indirectly aided in this investigation.

In particular, he wishes to acknowledge the interest, help, and encouragement of Assistant Professor C. M. Sliepcevich, the chairman of the Doctoral Committee, Professor G. G. Brown, Associate Professor J. W. Freeman, Assistant Professor P. A. S. Smith, and Professor R. R. White. The assistance of Kameo Sugino and W. E. Henderson in obtaining some of the experimental data is greatly appreciated.

The author is indebted to the Shell Fellowship Committee for financial assistance during the academic year 1949-1950.

TABLE OF CONTENTS

	page
LIST OF TABLES	vi
LIST OF FIGURES	vii
NOMENCLATURE	viii
SUMMARY	1
INTRODUCTION	3
EXPERIMENTAL WORK	7
Equipment	7
Preliminary Work	9
Experimental Procedure	14
Experimental Data	15
DISCUSSION OF RESULTS	21
Theory of Rate Processes	21
Method of Correlation	30
CONCLUSIONS	34
APPENDIX	36
BIBLIOGRAPHY	52

LIST OF TABLES

		page
TABLE I	MATERIAL BALANCES	13
TABLE II	EXPERIMENTAL DATA	18
TABLE III	SPECIFICATIONS OF BUTANOL-1	41
TABLE IV	ORIGINAL EXPERIMENTAL DATA	46

LIST OF FIGURES

Figure		page
1	Pressure and Temperature Gradient Curve	5
2	Flow Sheet	8
3	Process Period Runs	10
4	Butraldehyde Reaction Interference	12
5	Experimental Initial Rate-Fugacity Curves	19
5-A	Catalyst Activity Curves	20
6	Theoretical Initial Rate-Fugacity Curves	31
7	Thermocouple No. 3., Calibration	38
8	Pressure Gauge Calibration	39
9	Karl Fischer Reagent Curve	42
10	Initial Rate Determination	50

NOMENCLATURE

A	component A
c_j	ratio of active area of the catalyst covered by an arbitrary component, denoted by subscript "j", to the total active area
c_1	ratio of vacant active area of the catalyst to the total active area
$[c_f]_j$	adsorption-equilibrium constant for component "j" on the catalyst surface
f	fugacity in atmospheres
F	feed rate in (# mols)/(hr.)
k_1	adsorption proportionality constant for component A
k_2	desorption proportionality constant for component A
k_3	proportionality constant for forward surface reaction
k_4	proportionality constant for reverse surface reaction
k_5	proportionality constant for component R desorption
k_6	proportionality constant for component R adsorption
k_7	proportionality constant for component S desorption
k_8	proportionality constant for component S adsorption
K	equilibrium constant for surface chemical reaction
r	rate in (# mols)/(hr.)(# catalyst)
r_1	rate of adsorption of component A
r_2	rate of desorption of component A
r_3	rate of forward surface reaction
r_4	rate of reverse surface reaction
r_5	rate of desorption of component R

r_6	rate of adsorption of component R
r_7	rate of desorption of component S
r_8	rate of adsorption of component S
r_0	initial rate
r_{net}	net rate of reaction
R	component R
S	component S
W	# catalyst
x	ratio of pound moles of butanol-1 fed which reacted to form butenes and water to pound moles of butanol-1 fed.

Subscripts

A	of component A
f	in terms of fugacity
i	at the interface of the catalyst and the main body of the gas stream
j	arbitrary component
R	of component R
S	of component S

SUMMARY

A study of the effect of pressure up to 7500 pounds per square inch on the initial heterogeneous rate of dehydration of butanol-1 over an alumina-silica catalyst at 750° Fahrenheit (± approximately one percent) is presented.

It was observed that the curve of rate of reaction versus pressure passed through a maximum at a pressure which was equivalent to a fugacity of 85 atmospheres of butanol-1.

Based on the law of mass action, the existance of a rate controlling step, and the similarity of the adsorption of reactant and products on the active catalyst surface, it was found that the rate of the surface reaction was controlling. This relationship may be theoretically expressed as follows:

$$r_0 = \frac{(k_3)\ [C_f]_A\ (f_A)}{\left[1 + [C_f]_A\ (f_A)\right]^2} \qquad (38$$

where r_0 is the initial heterogeneous reaction rate in (# mols)/(hr.)(# catalyst).

k_3 is the proportionality constant for the forward reaction.

$[C_f]_A$ is the adsorption-equilibrium constant for component A on the catalyst surface in reciprocal atmospheres.

f_A is the fugacity of component A (butanol-1) in atmospheres.

From the experimental data and the above assumptions the adsorption-equilibrium constant $[C_f]_A$ for butanol-1 on an

alumina-silica catalyst at 750° Fahrenheit (≤ approximately one percent) was found to be:

$$1.2 \times 10^{-2} \text{ atmospheres}^{-1}$$

INTRODUCTION

The study of the initial rate of dehydration of butanol-1 at a single temperature and over a wide range of pressure was undertaken to determine the rate controlling step (maximum resistance) in a heterogeneous, catalyzed, single fluid-phase reaction.

Previous experimental work in heterogeneous catalytic reactions have not stressed the use of initial rates and pressure, but rather have stressed the effect of time, temperature, feed rate, and concentration on conversion. While these latter variables are useful in studying the rate and order of chemical reactions, their usefulness in mechanism studies of heterogeneous, catalyzed reactions is limited.

The time of reaction cannot be directly measured in a flow reactor; therefore, it is not a convenient variable for correlation of rate data (8).

The effect of temperature on a reaction is of little value in the selection of reaction mechanisms since it usually is not possible to establish with certainty the probable mechanism (23). The effect of temperature, however, can be used in determining the apparent energies which are required to cause a reaction to take place (activation energy).

The effect of feed composition can be useful in mechanism studies (23), but it was not considered here because a feed, consisting of a pure component, was used. Dilution

of the feed presents the problem of separating the effects of the diluent itself from the effect of a change in concentration caused by the diluent (16). This difficulty outweighs the benefits obtained by the added variable.

The variable, rate of feed (mass space velocity), is limited in studying mechanisms in heterogeneous systems because isothermal operation can seldom be obtained at low feed rates. Since most all reactions are accompanied by an increase in enthalpy, either positive or negative, large temperature gradients will occur across the interface of the catalyst and the gas stream thereby making isothermal operation impossible. From the "j" factor correlation (4 and 23) it is possible to estimate the magnitude of the temperature and pressure gradients existing between the catalyst surface and the main body of the fluid phase. As shown in Figure 1, the heat and mass transfer gradients increase rapidly with decreasing feed rates. Therefore, to minimize these effects, experimental studies should be made at high feed rates.

The variable, degree of conversion, is suitable for mechanism studies only at low conversions. At high conversions where the products of the reaction are appreciable the reverse reaction occurs to a considerable extent. In the limit, at chemical equilibrium, the forward and reverse reaction rates proceed at equal velocities. However, when the amount of products is made vanishingly small, the effect of the reverse reaction becomes negligible. Thus, by only allowing small conversions

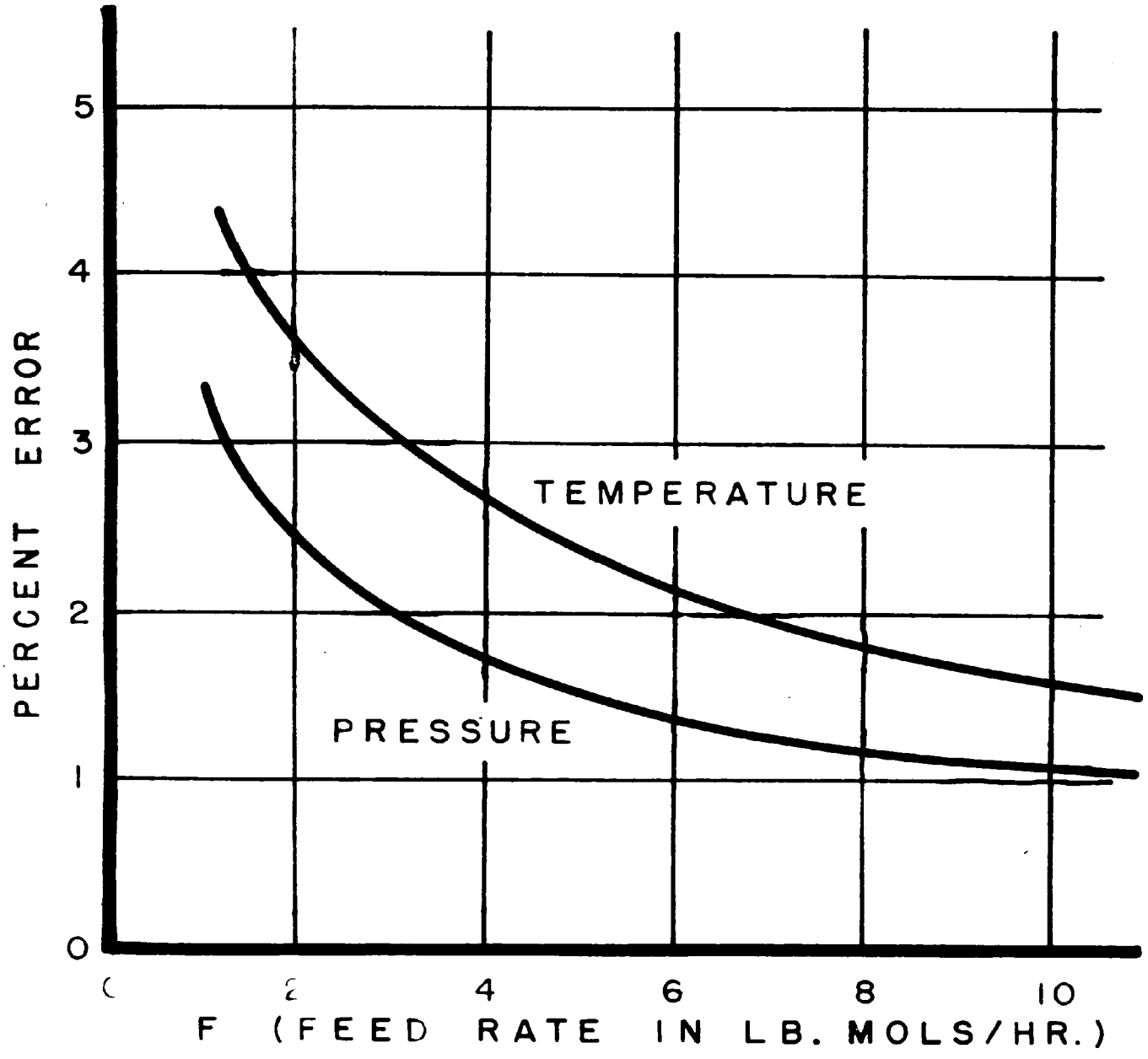

FIGURE 1. PRESSURE & TEMPERATURE GRADIENT CURVES

to take place in the reactor, it is possible, in effect, to study an actual reversible reaction, such as,

$$A \rightleftharpoons R + S \qquad (1$$

as if it were a simple, irreversible reaction,

$$A \longrightarrow R + S \qquad (1A$$

in which the reverse reaction need not be considered.

It should be observed that it is only necessary to study this reaction at low conversions or "initial conditions" and not necessarily at zero conversion. The allowable conversion is governed by the equilibrium condition of the reaction itself. For reactions which are essentially irreversible, higher conversions can be tolerated without interference from the reverse reaction.

Pressure is a useful variable in kinetic studies because it can produce, under certain conditions, unique effects on the rate of reaction and particularly on the initial rate. For this reason, only qualitative accuracy in the measurement of the variables, initial rate and pressure, is required, in most cases, for establishing the rate controlling step. Various investigators in the past (2, 3, 12, 15, 18) have considered the variable, pressure, in kinetic studies on heterogeneous reactions, but none have presented a systematic analysis or procedure for utilizing pressure in determining the rate controlling step. Recently, however, Yang and Hougen (23) have indicated the theoretical approach, but they report no experimental data. The present experimental work is

patterned after the theoretical recommendations of Yang and Hougen for the purpose of determining whether their procedure can be experimentally realized.

EXPERIMENTAL WORK

Before the final experimental data could be obtained the existing equipment had to be modified and a series of preliminary runs had to be made in order to establish the experimental technique. Measurements of the effect of pressure on the initial reaction rate were then made.

Equipment

A schematic flow diagram of the equipment is shown in Figure 2*. It is essentially the same equipment which was used in previous work (18). Several modifications were made in order to facilitate the experimental investigations. These changes consisted of the incorporation of a positive pressure feed system in order to confine the alcohol fumes, to give a positive pressure at the pump inlet, and to exclude oxygen from the system. A product handling system was devised and a chemical laboratory with complete analytical facilities was constructed to facilitate chemical analyses. A new preheater furnace was also installed.

* A description of this equipment is given in the Appendix Page 43.

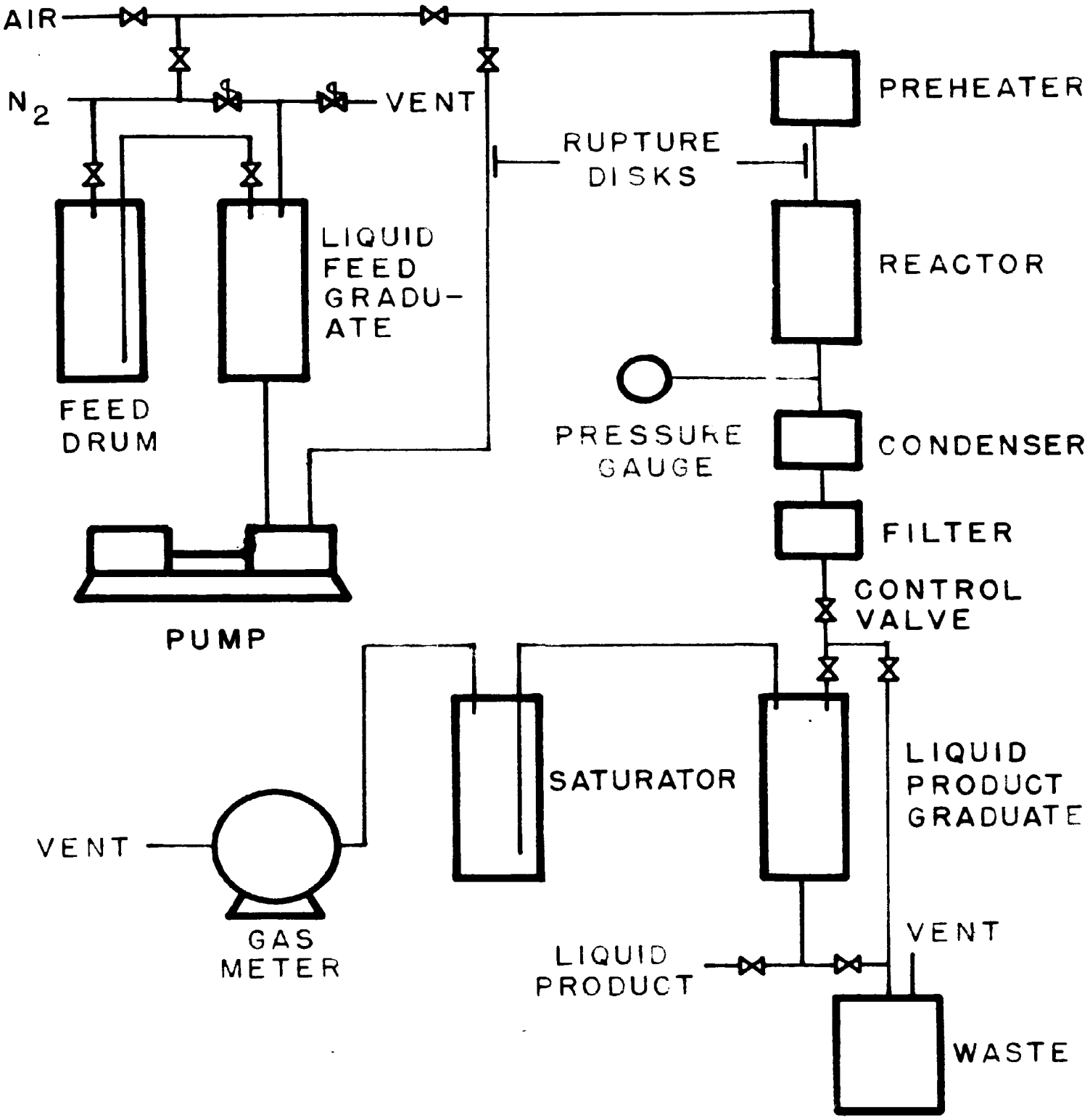

FIGURE 2. FLOW DIAGRAM

Preliminary Work

Several isothermal runs were made using an alumina-silica catalyst and operating at a temperature of 750° Fahrenheit at which previous work (18) had shown that the principle reaction was the dehydration of butanol-1 to butenes and water. The effect of time on the catalyst activity was determined as shown in Figure 3. Also included on this graph is the temperature variation during each period. Each process period, represented by a separate curve in Figure 3, was preceded by a reactivation period in which the carbon residue was burned off with air at about 1000° Fahrenheit.

From the relation of temperature and time in Figure 3 it was concluded that the control of temperature in the catalyst bed was within one percent, permitting essentially isothermal operation.

The relation of conversion and time in Figure 3 indicates that while a high initial conversion obtains, which drops off rapidly, a uniform conversion is eventually attained, which permits a mechanism study within a process (single reactivation) period. The plateaus of the conversion-time curves of Figure 3 are not reproducible. It is not possible, therefore, to make correlations between process periods since the catalyst activity does not remain constant.

The control of pressure in the flow reactor by a needle valve on the exit line proved to be simple, instantaneous in response, and free from trouble.

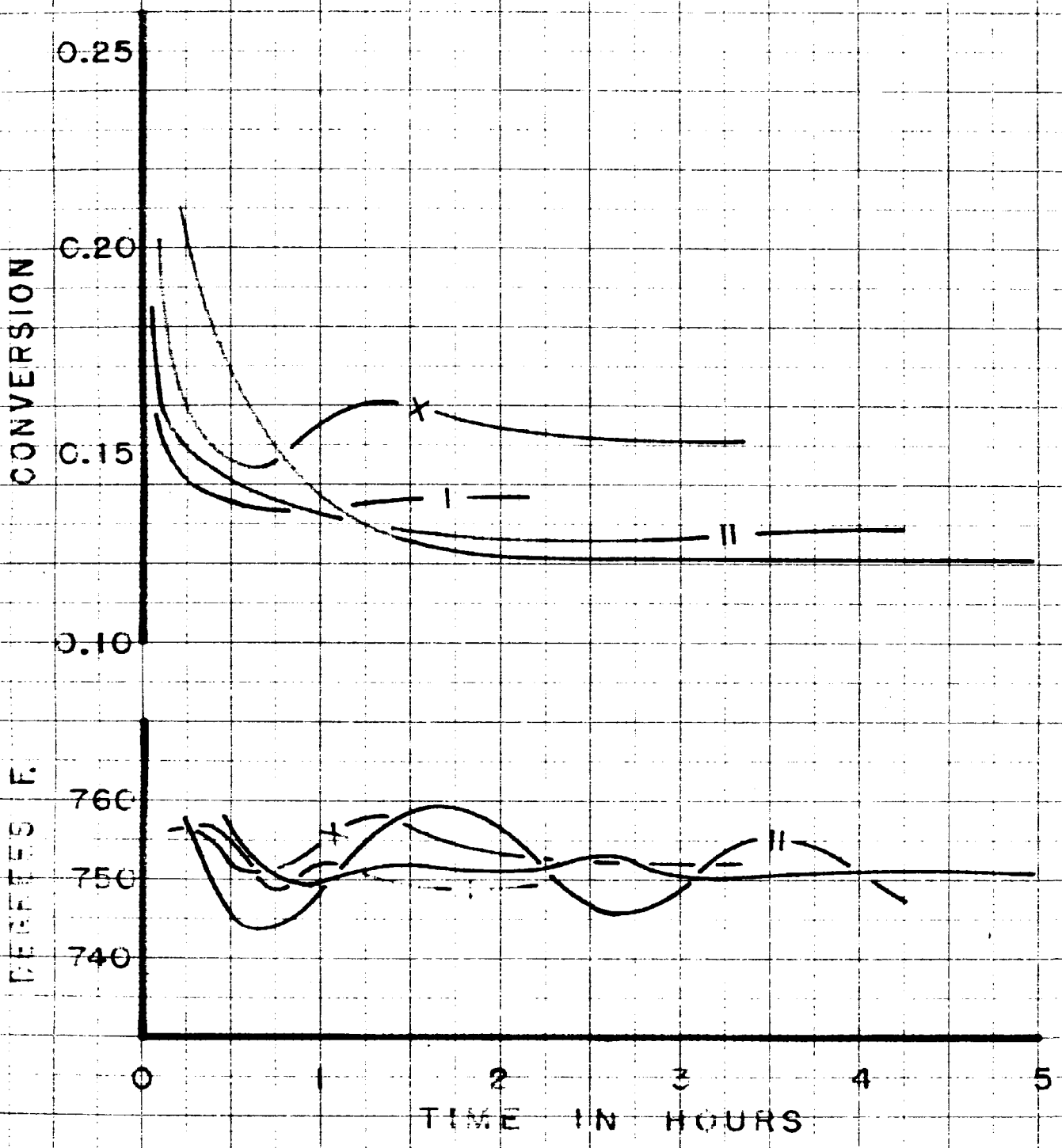

FIGURE 3. PROCESS PERIOD RUNS

Since the feed rate was found to remain constant at a particular pressure, steady-state operation was obtainable. A positive displacement, high pressure pump (Hills McCanna type HAJD - 3/8") proved satisfactory as long as a positive feed pressure of five inches of mercury on the inlet side was maintained.

The interference with the main catalytic dehydration reaction was observed to be principally the formation of aldehyde. However, the aldehyde reaction was shown to be present to such a small extent (Figure 4) that its influence on the main reaction could be neglected. The conversion to butyraldehyde may be due to the iron walls of the reactor since iron is known to promote the formation of aldehyde.

Thermal decomposition was previously shown by Ipatieff (12) to be negligible at the conditions of operation. This fact is confirmed again by the material balances for several runs (Table I) and by operation over long periods of time.

The possibility of ether formation was excluded since no ether could be detected by the infrared spectrograph at a wave length of 8.7 microns (17).

Previous work (21) indicated that for the conditions of operation the reverse reaction was negligible. Therefore, initial conditions should only have to be approximated.

From the above preliminary studies it was concluded that the main reaction was the dehydration reaction and that

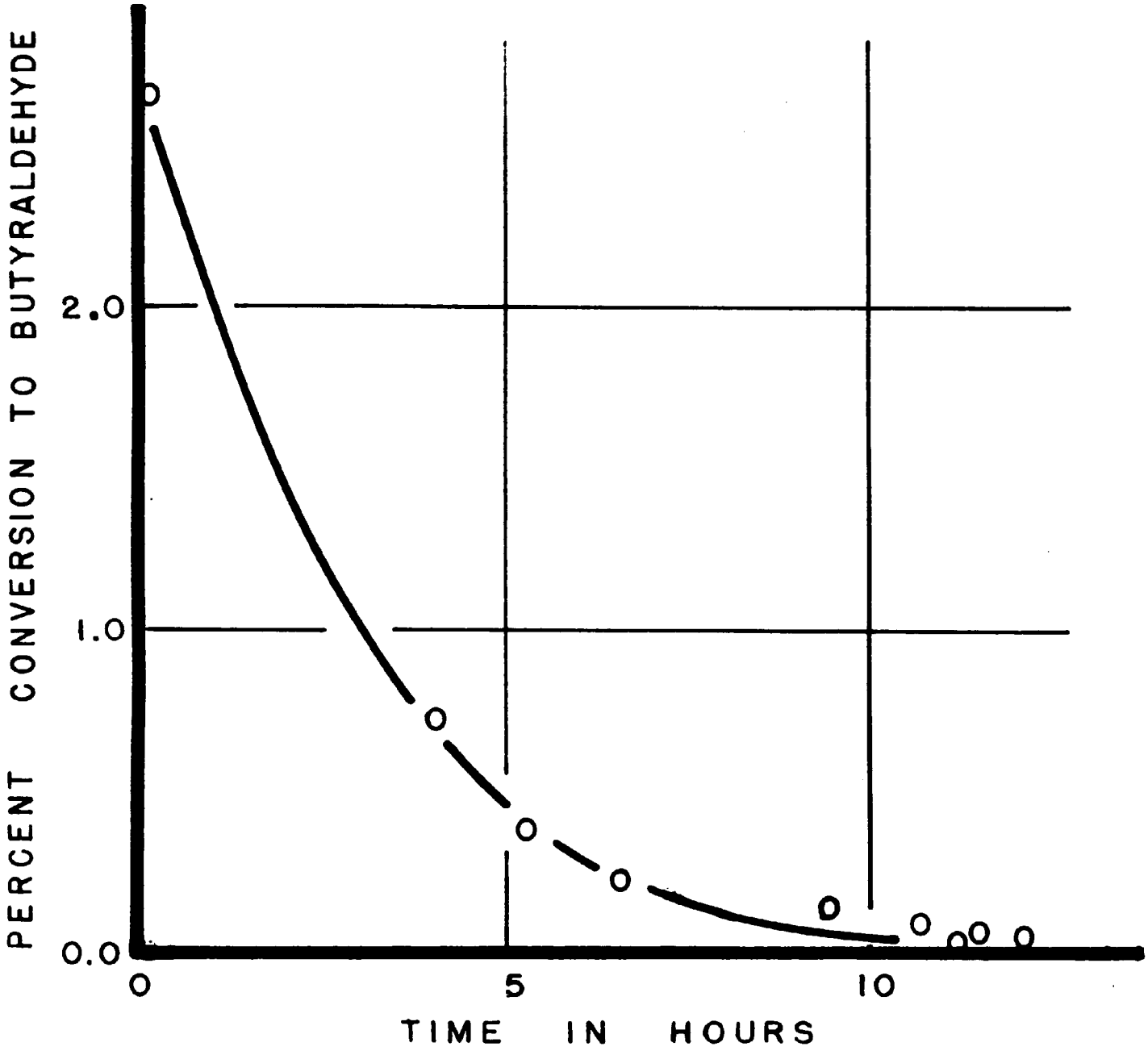

FIGURE 4. BUTYRALDEHYDE REACTION INTERFERENCE

TABLE I

Material Balances

Run #	Feed Rate (#)(hr.)	Liquid Product Rate (#)(hr.)	Gas Product Rate (#)(hr.)	△ (#)(hr.)	% Error
68	3.18	3.16	0.04	+ 0.02	+ 0.6%
69	2.96	2.93	<0.01	- 0.03	- 1.0
70	2.86	2.88	"	+ 0.02	+ 0.7
71	2.87	2.90	"	+ 0.03	+ 1.0
72	2.82	2.87	"	+ 0.05	+ 1.8
73	5.45	5.46	"	+ 0.1	+ 0.2
74	7.91	7.69	"	- 0.22	- 2.8
75	14.22	14.27	"	+ 0.05	+ 0.3
76	6.97	7.00	"	+ 0.03	+ 0.4
77	3.91	3.90	"	- 0.01	- 0.4
78	Discarded because of pump failure				
79	6.30	6.63	"	+ 0.33	+ 5.0
80	7.27	7.28	"	+ 0.01	+ 0.1
81	14.28	14.26	"	- 0.02	- 0.1
82	14.21	14.17	"	- 0.02	- 0.2
83	4.22	4.24	"	+ 0.02	+ 0.5
84	6.45	6.45	"	+ 0.00	0.0
85	4.78	4.74	"	- 0.04	- 0.6
86	1.92	1.89	"	- 0.03	- 1.5

Average material balance 100.2%

Average deviation ± 0.9%

an isothermal study of the effect of pressure at low conversions on the rate of reaction would be possible.

Experimental Procedure

The rate of the chemical reaction

$$A \rightleftharpoons R + S \qquad (1$$

can be measured by determining either the disappearance of A or the appearance of R or S. The precision with which the rate can be experimentally measured depends on the relative quantities of A, R, or S present. In the case of initial reaction studies where the disappearance of A is small, compared to the quantity of A present, the precision in determining the rate by measuring A will be low because the difference between two measured quantities of similar magnitude is determined. However, by measuring the appearance of R or S the precision in determining the initial rate approaches the precision of the analysis for R or S, which in this case was known to be satisfactory (Appendix page 40). For this reason, the determination of the initial rate of reaction was based on the determination of the water formed in the reactor rather than on the alcohol decomposed.

By measuring the conversion at three or more high mass velocities, or feed rates, the curve of conversion vs the ratio of the pounds of catalyst and the feed rate in pound moles per hour (W/F) was obtained. Since

$$F(x + dx) - Fx = rdW \qquad (2$$

where F is the feed rate in (# mols)/(hr.)

x is the conversion

r is the rate of reaction in (# mols)/(hr.)(# catalyst)

W is the pounds of catalyst

$$r = \frac{dx}{d(W/F)} \qquad (3$$

and $$r_o = \lim_{W/F \to 0} \frac{dx}{d(W/F)} = \text{Slope} \qquad (4$$

where r_o is the initial heterogeneous reaction rate. The details of experimentally determining the initial rate (slope) are given in the Appendix page 49.

Experimental Data

The experimental data are given in the Appendix, page 46, and summarized in Table II and Figure 5 and 5A.

The data were taken in four process periods, each of which consisted of a series of runs in which the effect of the independent variables pressure and W/F on conversion were investigated by two methods. In the first method the effect of pressure at three given space velocities were investigated by increasing the pressure by increments at one space velocity, decreasing the pressure by the same increments at a second space velocity, and finally increasing the pressure by the same increments at a third space velocity. In this manner the effect of time was introduced in a random manner. Any effect of time on the specific catalyst activity,

which is included in the term k_3 of equation 38 (page 29) will appear, therefore, as a random error in the relationship of initial rate and fugacity of component A.

In the second method the space velocity was increased by three increments at a given pressure followed by decreasing the space velocity by three increments at another pressure. This was continued over a range of pressures. In this manner the effect of time was likewise introduced in a random manner. By using these two methods for obtaining the experimental data, any change in catalyst activity with time could be readily detected.*

The value for k_3 for each experimental point was calculated from the theoretical equation which best fitted the experimental data (see equation 38, page 29) by substituting experimental values of the initial rate, the corresponding fugacity, and the adsorption-equilibrium constant into this equation. The values of k_3 for each data point could then be plotted versus the fugacity (Figure 5A).

The spread of the experimentally determined values for k_3 for each process period from an average value (a horizontal line) is a measure of all experimental errors plus errors due to random catalyst activity variations during the entire process period. Therefore, the

* An Introduction to Modern Statistical Methods by P. R. Rider, John Wiley and Sons, Inc., 1939, New York.

variation in catalyst activity with time must be less than the variation of k_3 from a mean value since part of this variation is due to experimental errors. From Figure 5A it can be concluded, therefore, that catalyst activity is essentially uniform.

Before each process period the catalyst bed was reactivated with air at about 1000° Fahrenheit in the same manner as in the preliminary work. In previous work (18) steam was used to regenerate the catalyst. However, from preliminary runs, it was found that reactivation could be accomplished by using air. Furthermore, as was shown in previous work, the use of steam in regeneration complicated the analysis of water in the products from which conversion was obtained. After passing air over the catalyst bed nitrogen was used to purge any oxygen remaining in order to prepare the catalyst bed for the next process period.

In process period four no reactivation preceeded the process period, but rather alcohol was allowed to remain in the bed at temperature. In this manner the effect of deactivation caused by coking was observed.

TABLE II

Experimental Data
on the
Dehydration of Butanol-1
over an
Alumina-Silica Catalyst
at 750°F

	$(x)(10^3)$	$(w/F)(10^3)$	$(x)(10^3)$	$(w/F)(10^3)$	$(x)(10^3)$	$(w/F)(10^3)$	r_0	p lb/in.^{2} (gage)	p corr. lb/in.^{2} (abs.)	(f/p^*)	f_A (atm)
	46	70	63	139	73	160	0.27	0	15	1	1.0
	60	74	77	107	85	123	0.51	500	465	0.88	27.9
1	67	77	83	98	112	100	0.76	1000	915	0.74	46.1
	75	91	100	170	273	425	0.76	4000	3845	0.43	112.
	79	113	83	125	221	365	0.52	7500	7315	0.46	229.
	65	139	50	107	38	71	0.41	200	200	0.95	13.6
	45	73	68	114	95	160	0.55	500	465	0.88	27.8
	100	163	85	128	59	81	0.55	1500	1415	0.64	61.5
2	58	91	64	146	129	205	0.61	3000	2885	0.47	92.2
	165	287	113	192	67	106	0.54	5000	4825	0.42	138.
	181	372	91	149	57	107	0.55	6000	5815	0.43	170.
	82	134	127	233	103	68	0.39	7500	7315	0.46	229.
	53	73	78	106	100	141	0.65	500	465	0.88	27.9
	67	75	94	113	115	150	0.69	1000	915	0.74	46.1
3	75	80	110	123	130	172	0.70	2000	1905	0.56	72.4
	103	90	153	149	168	238	0.64	4000	3845	0.43	112.
	27	71	38	105	41	113	0.32	300	300	0.92	19.1
	71	159	55	115	43	76	0.32	1200	1125	0.69	52.8
4	45	80	71	122	82	131	0.38	2000	1905	0.56	72.4
	92	208	67	149	45	93	0.40	3000	2895	0.47	92.5
	55	105	79	181	124	329	0.33	4800	4635	0.42	132.

* (9)

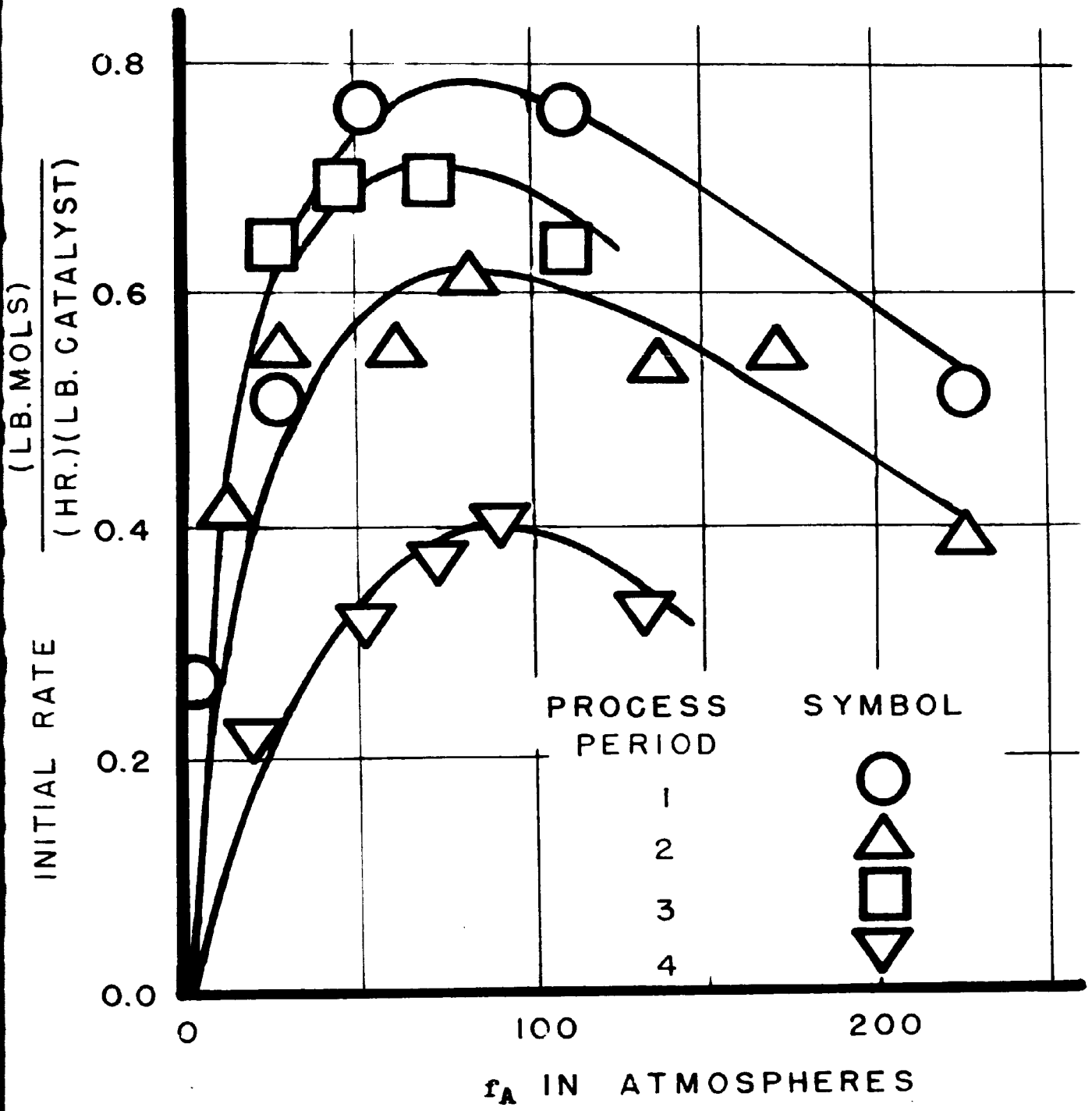

FIGURE 5. EXPERIMENTAL INITIAL RATE — FUGACITY CURVES

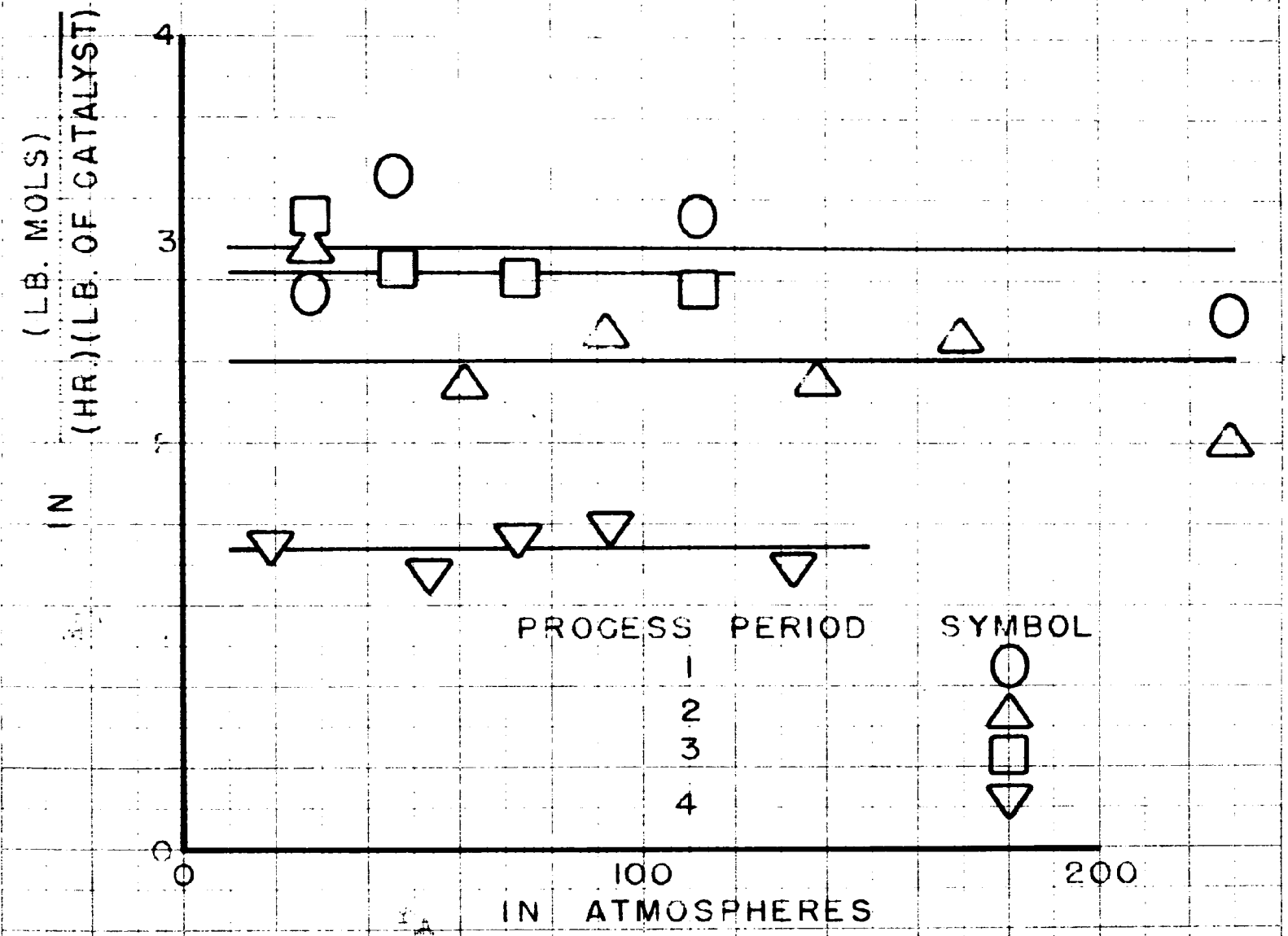

FIGURE 5-A CATALYST ACTIVITY CURVES

The initial reaction rate was determined by measuring the slope of the curve of conversion vs the ratio of the mass of catalyst and feed rate as given in the preceding section.

The total pressure, which is the pressure of butanol-1 for the initial conditions, was converted to the fugacity of butanol-1 with the aid of generalized fugacity coefficient charts (9) using the critical properties of butanol-1.

DISCUSSION OF RESULTS

In order to interpret the experimental data which were obtained during this investigation, a reaction rate theory based on the mass action law and Langmuir's adsorption theory was postulated, and the experimental results were correlated in terms of this theory. From this correlation it was possible to determine the rate controlling step and to compute the adsorption equilibrium constant for butanol-1 on the alumina-silica catalyst at 750° Fahrenheit.

A Theory of Reaction Rates

The following derivation of an applicable theory was taken from Glasstone (6) and from papers by Langmuir (13 and 14) and is similar to that of Hougen and Watson (8). It is important that all assumptions involved in the theory of rate processes be clearly understood before an interpretation of the experimental results is attempted.

The first assumption is the applicability of the law of mass action or "active mass" to catalyzed reactions (6, 13, and 14). This assumption appears logical, at present, since the law of mass action is the only concept that has been developed to explain rate processes.

The second assumption is that only the rate of one step out of a series of steps is of importance, or is controlling, under the conditions of operation. This assumption is based on the idea that in a sequence of events the individual rates of each event will be of a different order of magnitude. The minimum requirement of this assumption is that only the step having the maximum resistance need be of a different order of magnitude from the other steps at the conditions of operation.

The third assumption assumes that adsorption of the gas on the active catalyst surface occurs in the same manner for both reactant and product gases (8, 13, and 14). Granting these basic assumptions, it is possible to interpret the experimental data in the light of a reaction rate theory.

From the second assumption, which assumes that the heterogeneous, catalyzed gas-phase dehydration of butanol-1 occurs in a sequence of steps, five consecutive steps can be postulated:

1. Mass transfer of butanol-1 to the catalyst interface from the main gas stream.

2. Adsorption of butanol-1 on the active catalyst surface.

3. The chemical reaction of adsorbed butanol-1 to form adsorbed butenes and water.

4. The desorption of the products from the active surface to the interface.

5. Mass transfer of the products from the interface to the main gas stream.

All five of these steps are considered as reversible processes. Since one of these five steps is assumed to have a large resistance, with respect to the others, the remaining four will necessarily approach equilibrium in respect to their individual specific reaction velocities. However, the net rate of reaction must necessarily be the same for each step of the five consecutive steps when the entire system is in a steady-state condition.

The effects of mass transfer, steps one and five above, can usually be eliminated as rate controlling steps by keeping their rate at a maximum value by operating at high mass velocities (23). The equations for the remaining steps of adsorption, surface reaction, and desorption can be derived from the above assumptions and considerations.

If adsorption of the reactant is the rate controlling step, the rates of the surface reaction and desorption of products are assumed to be essentially in a state of equilibrium. Then, for the adsorption of component A (butanol-1)

$$r_1 = (k_1)\ (f_{A1})\ (c_1) \qquad (5$$

where r_1 is the rate of adsorption in (# mols)/(hr.)(# catalyst)

k_1 is the proportionality constant for the adsorption of component A

f_{A1} is the fugacity of component A at the interface

c_1 is the ratio of vacant active area to total active area

For the reverse reaction of desorption of component A

$$r_2 = (k_2)\ (c_A) \qquad (6$$

where r_2 is the rate of desorption of component A

k_2 is the proportionality constant for the desorption of component A

c_A is the ratio of active area covered by component A to the total active area

If equilibrium exists,

$$(k_1)\ (f_{A1})\ (c_1) = (k_2)\ (c_A) \qquad (7$$

or

$$\frac{k_1}{k_2} = \frac{c_A}{(f_{A1})\ (c_1)} = [c_f]_A \qquad (8$$

where $[c_f]_A$ is the adsorption-equilibrium constant (in terms of fugacity) for the adsorption of component A on the catalyst.

However, at any time, the net rate of reaction is,

$$r_{net} = r_1 - r_2 = (k_1)(f_{A1})\ (c_1) - (k_2)\ (c_A)$$

$$= k_1 \left[(f_{A1})\ (c_1) - \frac{c_A}{[c_f]_A}\right] \qquad (9$$

Since the surface reaction is essentially at equilibrium, the rate of the forward surface reaction is:

$$r_3 = (k_3)\ (c_A)\ (c_1) \qquad (10$$

where r_3 is the rate of the forward reaction

k_3 is the proportionality constant for the forward surface reaction.

The rate for the reverse surface reaction is given by:

$$r_4 = (k_4)\ (c_R)\ (c_S) \qquad (11$$

where r_4 is the rate of the reverse reaction

k_4 is the proportionality constant for the reverse surface reaction

c_R is the ratio of the active area covered by component R to the total active area.

c_S is the ratio of the active area covered by component S to the total active area

At equilibrium,

$$(k_3)\ (c_A)\ (c_1) = (k_4)\ (c_A)\ (c_S) \qquad (12$$

or

$$\frac{k_3}{k_4} = \frac{(c_R)\ (c_S)}{(c_A)\ (c_1)} = K \qquad (13$$

where K is the equilibrium constant for the surface reaction. (It should be noted that this constant is not the same as the ordinary chemical equilibrium constant for the reversible reaction since it includes the effect of the active surface of the catalyst.)

Since the desorption of the products is assumed to have essentially reached equilibrium, the rate of desorption of component R is:

$$r_5 = (k_5)\ (c_R) \qquad (14$$

where r_5 is the rate of the desorption of component R

k_5 is the proportionality constant for the desorption of component R

For the rate of adsorption of product R,

$$r_6 = (k_6)\ (f_{R1})\ (c_1) \qquad (15$$

where r_6 is the rate of adsorption of component R

k_6 is the proportionality constant for the adsorption of component R

At equilibrium the Langmuir isotherm equation can be written as:

$$(k_5)\ (c_R) = (k_6)\ (f_{R1})\ (c_1) \qquad (16$$

which can be rearranged,

$$\frac{k_6}{k_5} = \frac{c_R}{(f_{R1})\ (c_1)} = [c_f]_R \qquad (17$$

where $[c_f]_R$ is the adsorption-equilibrium constant for component R on the active catalyst surface.

For the desorption of component S from the catalyst,

$$r_7 = (k_7)\ (c_S) \qquad (18$$

where r_7 is the rate of desorption of component S

k_7 is the proportionality constant for the desorption of component S

For the reverse process of adsorption of component S:

$$r_8 = (k_8)\ (f_{S1})\ (c_1) \qquad (19$$

where r_8 is the rate of adsorption of component S on the catalyst

k_8 is the proportionality constant for the adsorption of component S

At equilibrium, for component S,

$$(k_7)\ (c_S) = (k_8)\ (f_{S1})\ (c_1) \qquad (20$$

or

$$\frac{k_8}{k_7} = \frac{c_S}{(f_{S1})\ (c_1)} = [C_f]_S \qquad (21$$

where $[C_f]_S$ is the adsorption-equilibrium constant for component S on the catalyst.

Since from Langmuir's equations (13 and 14),

$$c_1 + c_A + c_R + c_S = 1 \qquad (22$$

the equation for the net rate of reaction can be obtained by combining equations 9, 13, 17, 21, and 22; thus,

(23

$$r_{net} = k_1 \frac{f_{A1} - \dfrac{[C_f]_R\ [C_f]_S\ (f_{R1})\ (f_{S1})}{(K)\ [C_f]_A}}{1 + \dfrac{[C_f]_R\ [C_f]_S\ (f_{R1})\ (f_{S1})}{K} + [C_f]_R\ (f_{R1}) + [C_f]_S\ (f_{S1})}$$

For the initial conditions investigated several simplifications can be made in equation 23,

$$\lim_{\frac{W}{F} \to 0} f_{R1} = 0 \qquad (24$$

$$\lim_{\frac{W}{F} \to 0} f_{S1} = 0 \qquad (25$$

$$\lim_{\frac{W}{F} \to 0} f_{A1} = f_A \qquad (26$$

Thus, combining equations 23, 24, 25, and 26, the initial rate of reaction is,

$$r_0 = (k_1) \quad (f_A) \tag{27}$$

This equation is represented qualitatively in Figure 6-a.

When the surface reaction is the rate controlling step, it is assumed that the rates of adsorption and desorption of the reactants and products each have essentially attained equilibrium.

Then, for the adsorption of component A:

$$r_1 = (k_1) \quad (f_{Ai}) \quad (c_1) \tag{28}$$

and for the reverse reaction

$$r_2 = (k_2) \quad (c_A) \tag{29}$$

At equilibrium the equation for Langmuir's isotherm can be written:

$$(k_1) \quad (f_{Ai}) \quad (c_1) = (k_2) \quad (c_A) \tag{30}$$

or

$$\frac{k_1}{k_2} = \frac{c_A}{(f_{Ai}) \quad (c_1)} = [c_f]_A \tag{31}$$

For the surface reaction the forward rate is:

$$r_3 = (k_3) \quad (c_A) \quad (c_1) \tag{32}$$

and the reverse rate is:

$$r_4 = (k_4) \quad (c_R) \quad (c_S) \tag{33}$$

If equilibrium were attained,

$$(k_3) \quad (c_A) \quad (c_1) = (k_4) \quad (c_R) \quad (c_S) \tag{34}$$

$$\text{or,} \qquad \frac{k_3}{k_4} = \frac{(c_R)\ (c_S)}{(c_A)\ (c_1)} = K \qquad (35$$

When chemical equilibrium does not obtain, the net rate of the surface reaction is:

$$r_{net} = (k_3)\ (c_A)\ (c_1) - (k_4)\ (c_R)\ (c_S) = k_3 \left[(c_A)(c_1) - \frac{(c_R)(c_S)}{K} \right] \qquad (36$$

From equations 21, 22, 31, 35, and 36 the net rate of reaction can be written in terms of measurable quantities as:

$$r_{net} = k_3 \frac{[c_f]_A\ (f_{A1}) - [c_f]_R\ [c_f]_S \frac{(f_{R1})\ (f_{S1})}{K}}{\left[1 + [c_f]_A\ (f_{A1}) + [c_f]_R\ (f_{R1}) + [c_f]_s (f_{S1})\right]^2} \qquad (37$$

By combining equations 24, 25, 26, and 37 the rate for the initial conditions can be written as:

$$r_0 = \frac{(k_3)\ [c_f]_A\ (f_A)}{\left[1 + [c_f]_A\ (f_A)\right]^2} \qquad (38$$

Equation 38 is represented in Figure 6-b.

When the desorption of the products is the rate controlling step, the rates of adsorption and desorption of the reactant and the surface reaction are assumed to be essentially at equilibrium. Thus, if the desorption of component R is the rate controlling step the rate of desorption for component R is:

$$r_5 = (k_5)\ (c_R) \qquad (39$$

For the adsorption of component R

$$r_6 = (k_6)\ (f_{R1})\ (c_1) \qquad (40$$

If equilibrium existed

$$(k_5)\ (c_R) = (k_6)\ (f_{R1})\ (c_1) \qquad (4$$

$$\text{or,}\quad \frac{k_6}{k_5} = \frac{c_R}{(f_{R1})\ (c_1)} = [C_f]_R \qquad (42$$

Since equilibrium does not exist the net rate of desorption is:

$$r_{net} = (k_5)(c_R) - (k_6)(f_{R1})(c_1) = k_5\left[c_R - [C_f]_R (f_{R1})(c_1)\right] \qquad (43$$

By combining equations 21, 22, 31, 35, and 43 the net rate of reaction when the desorption of component R is controlling is:

$$r_{net} = k_5 \frac{\dfrac{(K)\ [C_f]_A\ (f_{A1})}{[C_f]_S\ (f_{S1})} - [C_f]_R\ (f_{R1})}{\left[1 + [C_f]_A\ (f_{A1}) + \dfrac{(K)\ [C_f]_A\ (f_{A1})}{[C_f]_S\ (f_{S1})} + [C_f]_S\ (f_{S1})\right]} \qquad (44$$

Combining equations 24, 25, 26, and 44 and multiplying by $\frac{f_{S1}}{f_{S1}}$ the initial conditions for equation 44 becomes:

$$r_0 = k_5 \qquad (45$$

This equation is represented qualitatively in Figure 6-c.

Method of Correlation

For the overall reaction studied a series of five steps has been postulated.

1. Mass transfer of the reactant, component A, from the main body of the gas phase to the interface of the catalyst.

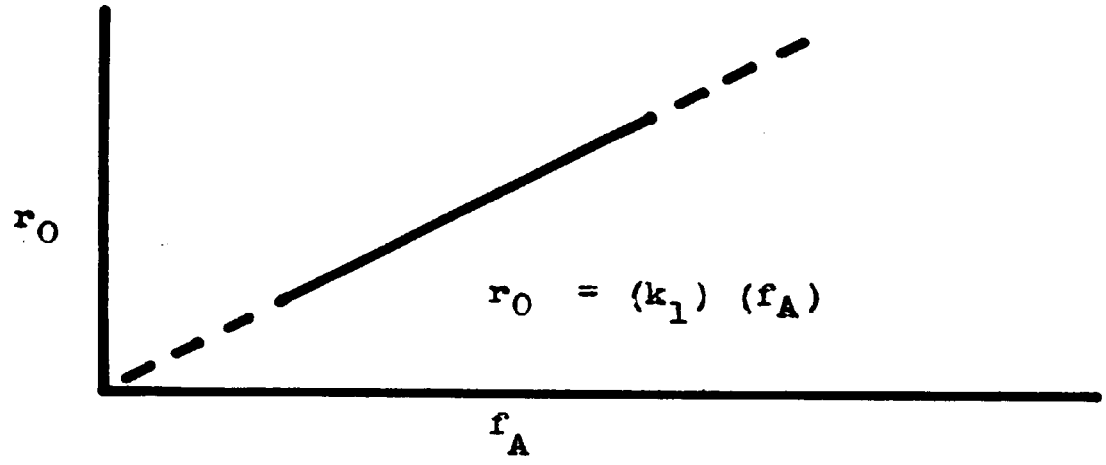

(27

a. ADSORPTION OF REACTANT CONTROLLING

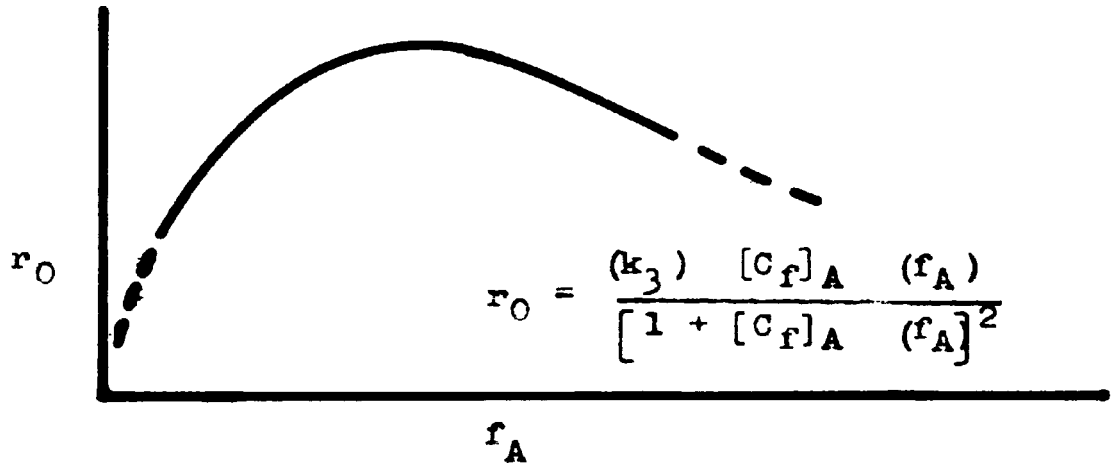

(38

b. SURFACE REACTION CONTROLLING

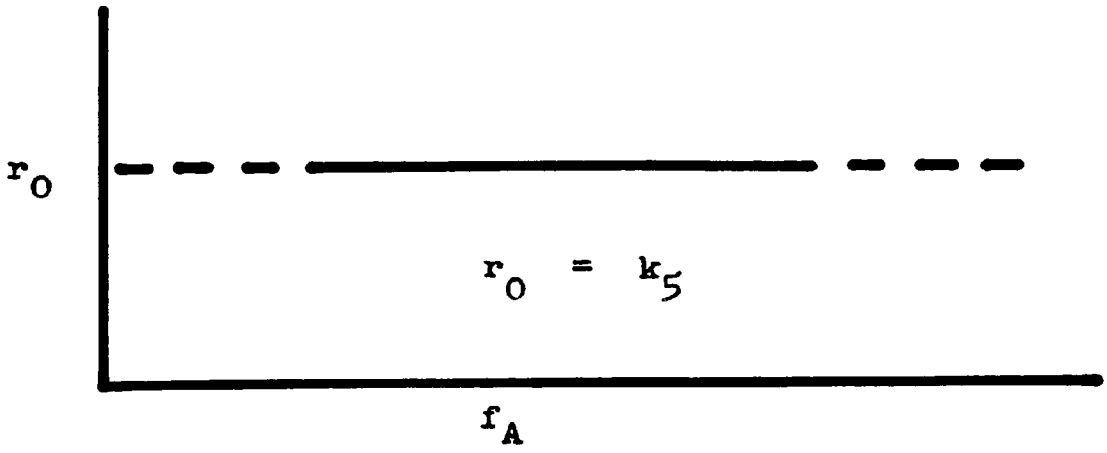

(45

c. DESORPTION OF PRODUCTS CONTROLLING

FIGURE 6. THEORETICAL INITIAL RATE — FUGACITY CURVES

2. Adsorption of the reactant, component A, on the catalyst.

3. Chemical reaction on the catalyst surface.

4. Desorption of the products, components R and S, from the catalyst to the interface.

5. Mass transfer of the products, components R and S, from the interface to the main gas stream.

It has been assumed that the rates of these five steps differ from each other, and as a minimum condition the rate of the step of maximum resistance is different from the others for the conditions studied.

Since mass transfer, steps one and five, are not likely to be controlling, only steps two, three, and four are possibly rate controlling steps. The relation of initial rate and fugacity of component A has been derived in the previous section, and the three possibilities are represented in Figure 6.

From Figure 5 the initial rate was shown to increase with fugacity of component A up to approximately 85 atmospheres. Therefore, the desorption of component R could not be a controlling step.

By extending the range of the fugacity of component A beyond 85 atmospheres to about two hundred atmospheres it was possible to eliminate the adsorption of component A as a possible rate controlling step (compare Figures 6-a and 6-b).

Since both the experimental data (Figure 5) and equation 38. (Figure 6-b) exhibited the same type of relationship, it was concluded that the surface reaction was the rate controlling step, independent of the activity of the catalyst. Furthermore, since the maximum point for all the curves of Figure 5 occurs at the same fugacity, it would appear that any difference in the activity of the catalyst may be due only to a variation in the active catalyst area per unit mass. It can be shown that the abscissa of the maximum point of the curves of Figure 5 is the reciprocal of the adsorption equilibrium constant for butanol-1 on the alumina-silica catalyst at 750°F in the following manner:

From equation 38,

$$r_0 = \frac{(k_3)\ [C_f]_A\ (f_A)}{\left[1 + [C_f]_A\ (f_A)\right]^2} \cdot \qquad (38$$

Applying the conditions for a maximum point

$$\frac{dr_0}{df_A} = \frac{\left[1 + [C_f]_A\ (f_A)\right](k_3)\ [C_f]_A - (2)\ (k_3)\ [C_f]_A^2\ (f_A)}{\left[1 + [C_f]_A\ (f_A)\right]^3} = 0. \qquad (46$$

Thus, $f_A = \frac{1}{[C_f]_A}$, and $r_0 = \frac{k_3}{4}$ at the maximum point. (47

From Figure 5, then, the adsorption equilibrium constant, $[C_f]_A$ is equal to 1.2×10^{-2} atmospheres $^{-1}$ or f_A at the maximum is 85 atmospheres.

CONCLUSIONS

1. By studying the effect of pressure, over a wide range, on the initial rate of reaction, it is possible to determine experimentally by direct means the rate controlling step in a heterogeneous catalytic reaction. Since only the shape of the curve of pressure and initial rate are required, it is possible to measure rates approximating, but not equal to, the initial rate since the rates from the initial to the final (equilibrium) rate will form a family of similar curves, progressing asymtotically toward the abscissa (23). However, in order to measure the constants in the theoretical equation for the rate controlling step, the initial conditions should be approached as closely as possible.

2. An alumina-silica bead catalyst was found to have sufficient stability during a process period to permit a mechanism study.

3. The rate controlling step of the dehydration reaction of butanol-1 under the conditions investigated was found to be the surface reaction.

4. The value of the adsorption-equilibrium constant for butanol-1 on the catalyst at 750° Fahrenheit (± one percent) was found to be:

$$1.2 \times 10^{-2} \text{ atmospheres}^{-1}$$

5. The adsorption-equilibrium constant was found to be independent of catalyst activity, suggesting that the

change in activity was due only to a change in amount of active area per unit mass and not due to a change in the properties of the active area.

APPENDIX

Measurement of Temperature

Reactor temperatures were measured with the use of calibrated chromel-alumel thermocouples, an ice bath cold junction, and a Leeds & Northrup No. 8662 portable precision potentiometer. The couples were calibrated in the Sohma Laboratory using a NBS 6275 platinum-rhodium platinum couple as a primary standard (Figure 7). Several calibrations established that the error in measuring temperature was less than one percent.

Measurement of Pressure

Pressure was measured using a Bourdon type gauge covering a range from zero to ten thousand pounds per square inch gauge. The pressure gauge was calibrated on the dead weight tester in the Sohma Laboratory, and the calibration is given in Figure 8. To determine if pressure drop within the reactor itself was significant, air was forced through the reactor at the same volume rate as was used in the experiments. The pressure drop through the entire system was found to be only five inches of mercury; therefore, the pressure drop in the reactor could be neglected. Calculations of pressure drop for the catalyst bed also indicated that no pressure gradient existed that would require consideration.

The average precision for the calibration was about plus or minus twenty-five pounds per square inch.

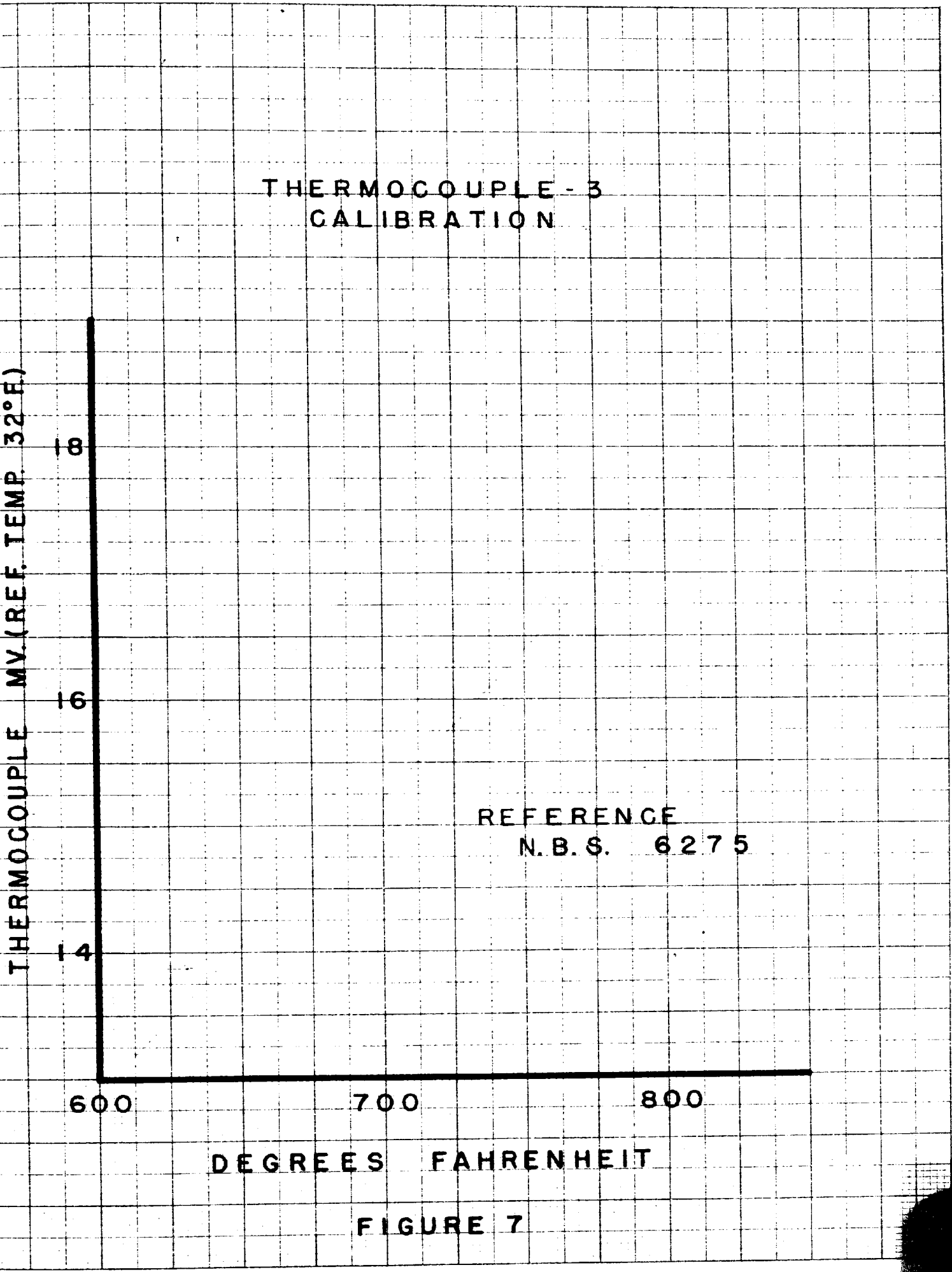
THERMOCOUPLE - 3
CALIBRATION
THERMOCOUPLE MV.(REF. TEMP. 32°F.)
18
16
14
REFERENCE
N.B.S. 6275
600
700
800
DEGREES FAHRENHEIT

FIGURE 7

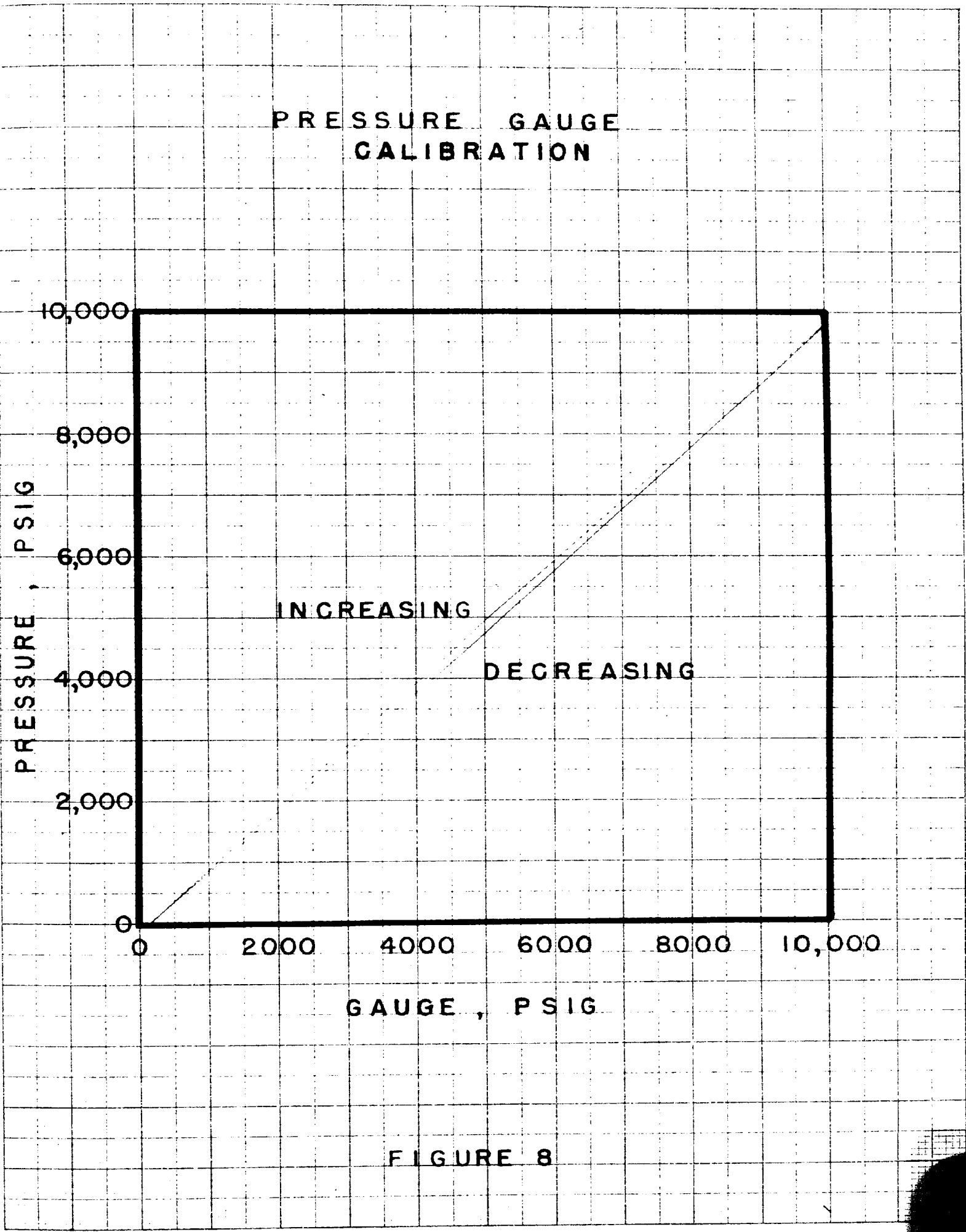
PRESSURE GAUGE
CALIBRATION
10,000
8,000
6,000
4,000
2,000
0
PRESSURE, PSIG
INCREASING
DECREASING
0
2000
4000
6000
8000
10,000
GAUGE, PSIG

FIGURE 8

Analysis

The analysis of the feed is given in Table III, and represents the average quality of the butanol-1 used.

The liquid product was analysed for water by the acetyl-chloride (19) and the Karl Fischer (20) methods. The Karl Fischer method was relied upon for most of the analytical work because of its greater precision and because it is specific for water. This method for water analysis is a direct volumetric analysis and is standardized against a known solution of water in methanol. A curve of its strength vs time (Figure 9) is used since the reagent is sensitive to air and moisture and depletes itself in time.

Traces of aldehyde were observed in the liquid product and were analyzed by precipitation with a solution of filtered 0.02 molar 2,4-dinitrophenylhydrazine in 2N. hydrochloric acid. The orange precipitate was washed with 2N. hydrochloric acid and finally with distilled water and was dried in a desiccator (10 and 11). The melting point of the precipitate was determined in a sealed glass tube and found to be 121-122° Centigrade, confirming that the aldehyde was a relatively pure sample of butyraldehyde (1). The quantitative method for determining the butyraldehyde consisted of weighing the precipitate from a sample of known weight in Gooch crucibles (10).

Dibutyl ether was shown to be absent in the liquid product when no adsorption occurred at a wave length of 8.7 microns in the infrared spectrograms of the product (17).

TABLE III

Specifications of Butanol-1

Source:

Commercial Solvents Corp.

Terre Haute, Ind.

Analysis:

1. Distillation Data

(Bar. 736.9 mm Hg at 24° C.)

First drop	115 C.
10 ml	115.1
30	115.6
70	116.1
100	116.4
200	116.7
300	117.0
350	117.8
395	119.5

2. Water Content

1. 0.08%
2. 0.06

Average: 0.07%

3. Aldehyde Test

1. Ammoniacal silver nitrate test - negative
2. 2,4-dinitrophenylhydrazine test - negative
3. Schiff's reagent test - negative

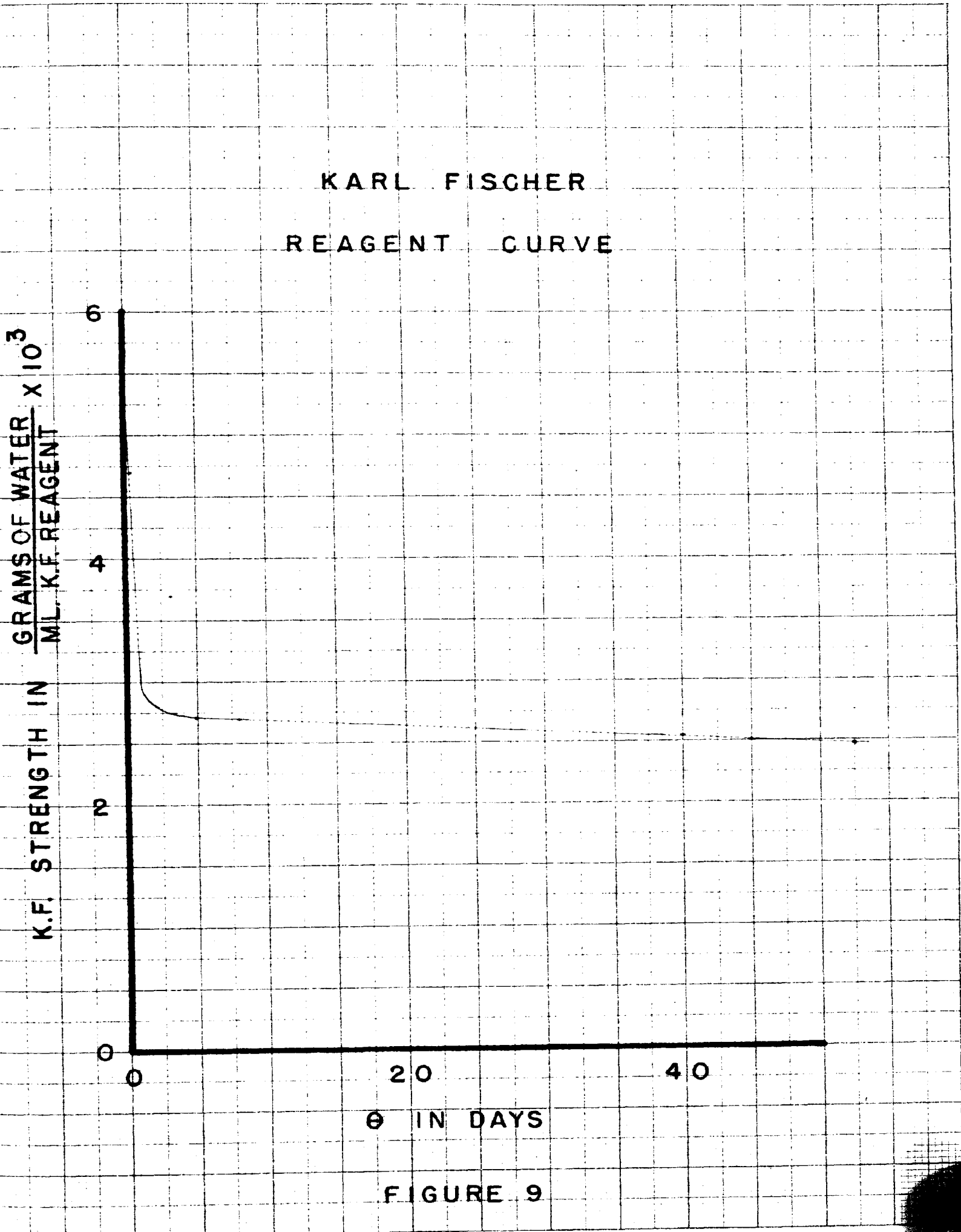
KARL FISCHER
REAGENT CURVE
K.F. STRENGTH IN GRAMS OF WATER / ML. K.F. REAGENT X 10^3
6
4
2
0
0
20
40
θ IN DAYS

FIGURE 9

Butenes were verified in the gas product by adsorption in sulfuric acid, gas gravity, and qualitatively by using the infrared and mass spectrometer.

Traces of hydrogen and unidentified saturated hydrocarbons were observed by using standard Orsatt gas analysis equipment.

Description of Equipment

A schematic flow diagram of the equipment has been shown in Figure 2, page 8. One 500 ml. graduated cylinder is used in the measurement of the feed from the pressurized feed drum to the high pressure pump (Hills McCanna type HADJ-3/8"). "Aminco" rupture disc assemblies are located downstream from the pump and are vented to the outdoors.

Two 30-foot coils of stabilized stainless steel tubing, type 321, 1/4-inch o.d. by 0.085-inch i.d., are located in an Eclipse pressed steel pot which serves as a preheater and is filled with DuPont Heat Treating Salt No. 1. The pot is heated by means of chromel resistance wire embedded in a fire brick furnace.

The steel tubing is connected to the top of the reactor using joints consisting of a 58° cone fitting into a 60° seat and coupled together by means of a pair of flanges and four 3/8-inch Bethlehem Steel studs.

The reactor consists of a forging of Uniloy 19-9 W-MO (high alloyed stainless steel) and is about three feet long.

The i.d. of the re ctor is 3/4-inch and its o.d. is 2-1/2 inches. The reactor is equipped with a Black, Sivalls, and Bryson special safety head of stainless steel which is also vented outdoors.

The bottom of the reactor is fitted with a 1/4-inch o.d. by 3/32-inch i.d. stainless steel thermocouple tube which extends the whole length of the reactor. A traveling thermocouple wire embedded in a two-holed ceramic insulator, permits measurements of the temperature over the entire length of the reactor.

Three separate radiant furnaces serve as reactor heaters. Each heater consists of chromel wire embedded in an alundum cement core. The heat input to each heater unit is controlled spearately by means of three "adjustavolts".

The salt pot and reactor furnaces are enclosed in a single housing. Fire brick and silocel are used as insulation. Each heater unit and the salt bath are equipped with chromel-alumel thermocouples.

The outlet from the bottom of the reactor includes a pressure gauge and condenser connection. The condenser consists of a coil of stabilized stainless steel tubing, 1/4-inch o.d. by 0.085-inch i.d. and a water box cooler. The condenser line extends to a filter and a stainless steel "Aminco" needle control valve by means of which the pressure on the entire apparatus is controlled.

Copper tubing, 1/4-inch o.d., connects the valve to the sampling manifold which provides for by-passing the product stream, measuring the liquid and gas rates, and sampling the liquid and gaseous products. This system is completely inclosed and vents outdoors.

The detailed specifications (including 120 pages and 24 figures) is presented in part 1 of reference 18.

TABLE IV

Original Experimental Data

(6.19 grams of catalyst)

Run No.	Feed Rate ml/min.	Liquid Product Rate ml/min.	Reactor Temp. °F. Upper	Middle	Lower	Pressure #/sq.in. gage	ml KF 2ml Product
85	134	135	748	752	754	0	6.0
86	68.2	68.6	746	750	751	0	8.13
87	59.1	62.5	753	751	749	0	9.00
88	98.5	99.	745	749	753	1000	12.1
89	67.7	68.5	750	750	750	1000	16.4
90	125	126	751	752	750	1000	9.8
91	129	130	748	751	752	500	8.7
92	88.3	89.6	749	749	747	500	11.1
93	77.0	77.2	749	750	747	500	12.6
94	22.3	22.7	755	750	748	4000	10.5
95	55.6	56.6	750	751	755	4000	17.6
96	104.	106.	745	750	753	4000	28.9
97	83.6	88.2	750	754	755	7500	33.6
98	75.9	77.6	745	749	754	7500	24.0
99	24.6	23.6	750	755	754	7500	9.7
124	67.8	68.2	745	750	752	200	8.02
125	88.5	90.3	745	751	752	200	6.09
126	134	137	745	752	753	200	4.42
127	130	131	749	753	754	500	5.54
128	82.5	83.2	756	758	758	500	8.32
129	59.2	60.4	752	757	751	500	11.52
130	58.0	58.4	755	752	750	1500	12.32
131	73.5	73.8	753	752	751	1500	10.45
132	116	118	758	758	750	1500	7.22
133	104	111	746	750	748	3000	6.81
134	64.7	65.5	746	747	748	3000	10.51

TABLE IV (Cont.)

Run No.	Feed Rate ml/min.	Liquid Product Rate ml/min.	Reactor Temp. °F. Upper	Middle	Lower	Pressure #/sq.in. gage	ml KF / 2ml Product
135	46.0	46.4	750	754	754	3000	15.86
136	32.8	32.5	749	753	748	5000	20.66
137	49.2	48.8	749	751	754	5000	14.16
138	89.1	90.5	750	753	756	5000	8.23
139	70.3	71.3	747	751	752	7500	9.81
140	40.5	40.6	749	752	753	7500	15.71
141	19.4	18.3	753	749	748	7500	25.46
142	25.3	22.3	745	749	745	6000	25.56
143	55.9	53.0	745	748	754	6000	22.76
144	88.3	88.6	750	751	751	6000	7.09
116	130	132	748	754	754	500	4.00
167	127	128	748	753	753	1000	5.01
168	119	121	748	749	752	2000	5.66
167	106	109	750	755	755	4000	7.71
170	86.4	87.8	751	755	753	7000	9.40
171	44.5	44.4	758	755	753	7000	18.20
172	63.6	63.5	752	756	751	4000	11.80
173	76.7	77.4	752	756	755	2000	8.35
174	83.7	84.0	753	758	757	1000	7.40
175	89.1	84.3	750	758	757	500	6.00
176	67.1	67.2	752	756	755	500	7.70
177	61.5	62.2	749	752	753	1000	8.90
178	53.0	53.6	746	752	751	2000	10.40
179	39.8	40.0	758	754	71	4000	16.70
180	19.2	18.7	758	759	751	7000	21.70

TABLE IV (Cont.)

Run No.	Feed Rate ml/min.	Liquid Product Rate ml/min.	Reactor Temp. °F. Upper	Middle	Lower	Pressure #/sq.in. gage	ml KF 2ml Product
106	59.8	60.2	749	751	751	1200	10.65
107	82.5	82.8	750	753	753	1200	8.31
108	125	133	751	754	755	1200	6.05
109	119	128	748	751	753	2000	6.25
110	77.5	78.4	751	756	756	2000	9.00
111	52.4	52.7	752	753	753	2000	12.25
112	45.7	43.8	749	752	751	3000	14.40
113	63.5	64.1	747	749	750	3000	10.06
114	102	104	748	749	751	3000	6.60
115	90.6	91.8	749	754	755	4800	8.10
116	52.4	52.8	747	748	747	4800	11.78
117	29.0	29.1	753	751	748	4800	19.90
118	66.5	66.8	750	753	751	300	6.20
119	90.2	92.0	747	751	754	300	5.10
120	133	133	749	753	755	300	4.10

Sample Calculation

From the experimental data the catalyst-feed rate ratio (W/F) is determined by multiplying the weight of catalyst in grams by the proper conversion factor and dividing by the product of the feed rate in ml/min. and the density of the feed in grams/ml. Thus for run 85:

$$\frac{(6.19 \text{ gram of catalyst})(1.24 \text{ Factor})}{(134 \text{ ml/min. Feed})(0.81 \text{ gram/ml})} = 70 \times 10^{-3}$$

$$W/F \text{ in } \frac{(\text{lb. catalyst})}{(\text{lb. mol. Feed/hr})}$$

The conversion of butanol is calculated by multiplying the Karl Fischer titration by the product rate in ml/min. and the proper conversion factor, and by dividing by the feed rate in ml/min. and the feed density in grams/ml. Thus for run 85:

$$\frac{(6.00 \text{ ml KF})\ (135 \text{ ml/min Prod.})\ (6.2\ 10^{-3} \text{ Factor})}{(.81 \text{ gram/ml})\ (134 \text{ ml/min Feed})} = 46 \times 10^{-3}$$

$$\text{conversion in } \frac{(\text{moles of Butanol converted})}{(\text{mole of Butanol Feed})}$$

The initial rate of reaction which is equal to the slope of a curve formed by a set of three calculated data points (x and W/F) at a given total pressure (Equation 4) is obtained by fitting a straight line to the curve at a point approaching a value of zero for W/F. Thus for runs 85, 86, and 87 the slope is equal to 0.27 lb. moles of Butene converted/hr. per lb. of catalyst Figure 10.

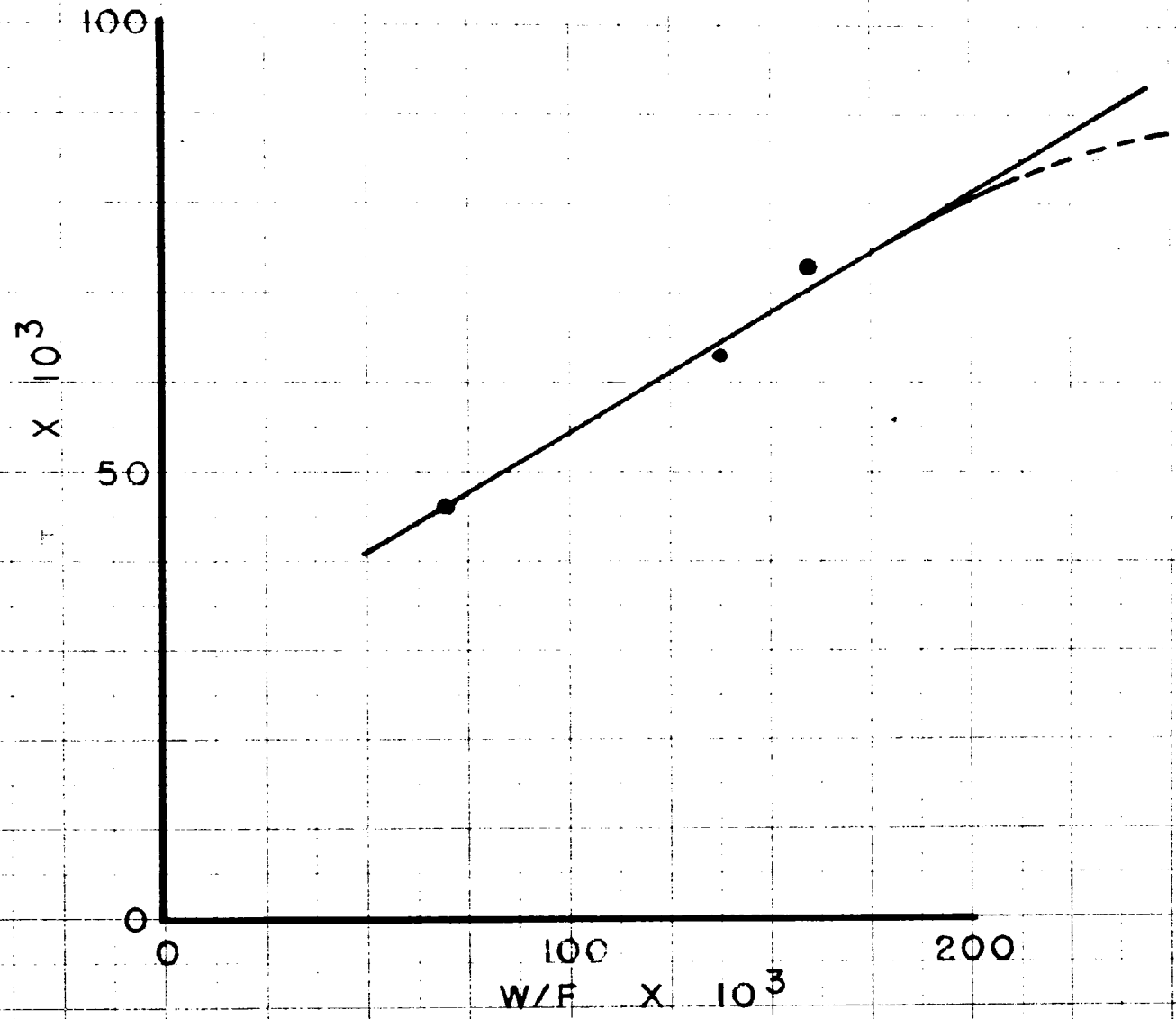

FIGURE 10 INITIAL RATE DETERMINATION

From all the experimental data the relation of initial rate and fugacity (pressure) of butanol is obtained (Figure 5).

BIBLIOGRAPHY

1. Allen, C.F.H., J.A.C.S. 52, 2955 (1930).

2. Atwood, K., Arnold, M.R., and Appel, E.G. Ind. Eng. Chem. 42, 1600 (1950).

3. Fawcett, E.W. and Gibson, R.O., J.C.S. 386 (1934).

4. Gamson, B.W., Thodos, G., and Hougen, O.A., Trans. Am. Inst. Chem. Engrs. 39, 1 (1943).

5. Getman, F.H. and Daniels, F., "Outlines of Theoretical Chemistry", p. 327, 6th ed. John Wiley and Sons, Inc., New York, (1937).

6. Glasstone, S., "Text-Book of Physical Chemistry", p. 805, D. Van Nostrand Company, Inc., New York (1940).

7. Hinshelwood, C.N., "The Kinetics of Chemical Change", Oxford, at the Clarenden Press (1940).

8. Hougen, O.A. and Watson, K.M., "Chemical Process Principles, III, Kinetics and Catalysis", John Wiley and Sons, Inc., New York, (1947).

9. Hougen, O.A. and Watson, K.M., "Chemical Process Principle Charts", John Wiley and Sons, Inc., New York (1946).

10. Iddles, H. A. and Jackson, C.E., Ind. Eng. Chem., 6, 454 (1934).

11. Iddles, H.A., Low, A.W., Rosen, B.D. and Hart, R.T., Ind. Eng. Chem., A. Ed., 11, 102-3 (1939).

12. Ipatieff, V.N., "Catalytic Reactions at High Pressures and Temperatures", The Macmillan Company, New York (1936).

13. Langmuir, I., J.A.C.S. 38, 2221 (1916).

14. Langmuir, I., J.A.C.S. 40, 1361 (1918).

15. Marek, L.F. and Flege, R.K., Ind. Eng. Chem. 24, 1428 (1932).

16. Millard, E.B., "Physical Chemistry for Colleges", p. 433-5, 5th Ed., McGraw-Hill Book Company, Inc. New York, (1941).

17. Randall, H.M., Fowler, R.G., Fuson, N., and Dangl, J.R., "Infrared Determination of Organic Structures", D. Van Nostrand Company, Inc., New York (1949).

18. Sliepcevich, C.M., Ph.D. Thesis, Chemical Engineering, University Microfilms, Ann Arbor, Michigan (1948).

19. Smith, D.M. and Bryant, W.M.D., J.A.C.S. 57, 841 (1935).

20. Smith, D.M., Bryant, W.M.D. and Mitchell, J. Jr., J.A.C.S. 61, 2407 (1939).

21. Studhalter, W. and Maurer, J.F., Unpublished Report, University of Michigan, Ann Arbor, Michigan (1947).

22. Wilke, C.R. and Hougen, O.A., Trans. Am. Inst. Chem. Engrs. 41, 445 (1945).

23. Yang, K.H., and Hougen, O.A. Ind. Eng. Chem. 46, 146 (1950).